ACS EARTH AND SPACE CHEMISTRY

# Formation of Protonated Glycine Isomers in the Interstellar Medium

Miguel Sanz-Novo, Antonio Largo,[ID] Pilar Redondo, and Carmen Barrientos*[ID]

Departamento de Química Física y Química Inorgánica, Facultad de Ciencias, Universidad de Valladolid, 47011 Valladolid, Spain

S Supporting Information

ABSTRACT: A computational study of protonated glycine isomers with $[H_6C_2O_2N]^+$ molecular formula has been carried out. All of them are possible products of the reaction between protonated hydroxylamine and acetic acid. All reaction processes that could form the $[H_6C_2O_2N]^+$ isomers considered in this work are exothermic except for those initiated by the most stable isomer of protonated hydroxylamine which give $CH_3CONH_2^+OH$ and $CH_3COHNOH_2^+$ isomers. The analysis of the potential energy surfaces corresponding to the reaction of protonated hydroxylamine and acetic acid has been focused on the most abundant products, namely, $CH_3CONH_2^+OH$, $CH_3COONH_3^+$, and $CH_3C(OH)^+ONH_2$, obtained from a previous chemical dynamics simulations study. From this analysis we found that even if the reactions of formation of the $CH_3COONH_3^+$ and the $CH_3C(OH)^+ONH_2$ isomers are exothermic processes, significant activation barriers were found in the paths leading to these products. The only exothermic process ($\Delta E = -23.9$ kcal mol^{-1} at the CCSD(T) level) with no net activation barrier was initiated by the high-energy isomer of protonated hydroxylamine, which leads to the $CH_3CONH_2^+OH$ isomer. Therefore, the formation of this isomer could be feasible under interstellar conditions from the reaction of the less stable isomer of protonated hydroxylamine and acetic acid. In addition, an analysis of their neutral counterparts, with $[H_5C_2O_2N]$ molecular formula, has been carried out. The relevant spectroscopic parameters for $[H_6C_2O_2N]^+$ and $[H_5C_2O_2N]$ isomers that could help in their laboratory or astronomical detection, by radioastronomy or infrared spectroscopy, are reported.

KEYWORDS: astrochemistry, interstellar medium general, interstellar medium molecules, interstellar medium structure, molecular data
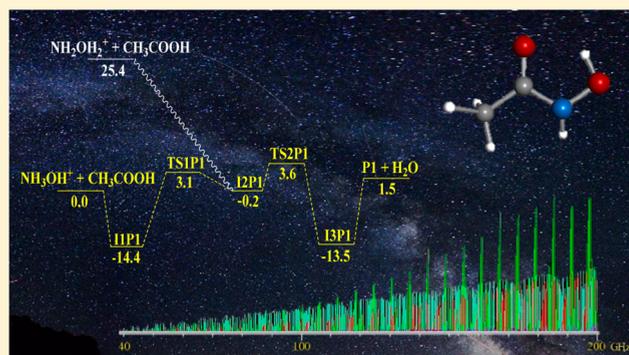
1. INTRODUCTION

Amino acids are essential components of living systems since they play a crucial role as building blocks of proteins. Amino acids were the first prebiotic molecules to be identified in the Miller experiment[1,2] from the reaction of simple organic molecules. On the other hand, taking into account their presence in some chondritic meteorites,[3-5] amino acids should be one of the easiest biomonomers to synthesize.[6] Despite several radioastronomical searches, so far the smallest amino acid, glycine, has not been conclusively identified in the interstellar medium (ISM).[7-10] However, recently, Altwegg et al.[11] have reported the presence of volatile glycine together with the precursor molecules methylamine and ethylamine in the coma of comet 67P/Churyumov-Gerasimenko. The observation of amino acids in the interstellar medium and in solar system bodies should be of crucial importance for revealing the chemistry that may have led to life's origin.[12]

There is a question as to whether glycine will ever be detectable even if present, given the difficulties for its possible detection in space.[13] One of these difficulties arises from its rotational spectrum features with relatively weak lines due to its large molecular partition function. Thus, search of the target transitions could be hindered by the emission of other molecules. Second, amino acids are highly susceptible to UV photodestruction and they will likely be destroyed during the lifetime of a typical interstellar cloud.[12] Consequently, they only survive in shielded environments. Finally, from a chemical-physics point of view, it might happen that efficient synthetic routes for the production of amino acids under interstellar conditions do not exist.

In this regard, exothermic ion–molecule reactions between positive ions and neutral molecules play a crucial role in the synthesis of organic interstellar molecules in the gas phase[14] since these processes tend to have no activation energy barriers. In particular, the feasibility of the gas-phase formation of protonated glycine from the reaction of acetic acid and protonated hydroxylamine was studied by Bohme and co-workers.[15,16] Both reactants are either detected or plausible interstellar molecules. Acetic acid was detected in the 3 mm region toward the massive star-forming region Sgr B2(N-

67 LMH)[17] as well in the additional hot core source W51e2.[18] So
68 far, hydroxylamine has not been detected in space but it is
69 considered a likely target of detection with ALMA.[19] N-bearing
70 molecules are precursors of prebiotic molecules, and among
71 them hydroxylamine appears to be one of the best candidates.
72 It is considered to be one of the main precursors in the
73 formation of amino acids in the interstellar medium. The
74 search for hydroxylamine in space has been devoted a lot of
75 attention in the most recent years, and many theoretical and
76 experimental studies have been focused on the processes of
77 formation of this compound. The chemical diversity and
78 complexity found in space could be explained as the result of
79 gas, grain, and gas−grain interactions in dense interstellar
80 clouds. In the most recent years, the study of surface processes
81 has received a growing interest in finding an alternative to gas-
82 phase reactions and also in understanding the composition of
83 icy mantles. In space, some species are formed from dust grains
84 mantles. In this context, from different laboratory experimental
85 studies[19−23] it was concluded that hydroxylamine could be
86 formed easily in solid phase and then it could desorb through a
87 temperature-induced process into the gas phase. Recently,
88 Jonusas and Krim[24] have reported a possible answer to the
89 nondetection of hydroxylamine trying to make sense of the
90 inconsistency between the high abundances of hydroxylamine
91 found in experimental studies and its nondetection in
92 astronomical sources. From a detailed study of the thermal
93 desorption mechanism, the authors concluded that the process
94 of heating of $NH_2OH−H_2O$ ices that led to a decomposition
95 of hydroxylamine into HNO, NH_3, and O_2 could reduce
96 considerably the abundance of hydroxylamine molecules
97 releasing in the gas phase. This thermal desorption mechanism
98 might be the primary explanation for the nondetection, so far,
99 of hydroxylamine in space. However, the presence of this
100 species in interstellar medium remains an open topic, and it
101 cannot be discarded as reactant for plausible interstellar
102 processes.
103   From their selected-ion flow tube (SIFT) experiments,
104 Bohme et al.[15,16] demonstrated the gas-phase ionic syntheses
105 of glycine from smaller molecules found in space. Specifically,
106 the authors[15,16] concluded that protonated glycine could be
107 formed by the reaction of the most energetic form of
108 protonated hydroxylamine, $NH_2OH_2^+$ and acetic acid. When
109 the reaction started from the lower energy form of protonated
110 hydroxylamine, NH_3OH^+, only clusters with carboxylic acids
111 were formed. These studies were very interesting, since the
112 formation of precursors of glycine was reported. Based on
113 those promising results, we carried out a computational study
114 of the reactions of ionized and protonated hydroxylamine with
115 acetic acid.[25] From the study, we concluded that the reaction
116 of the most stable protonated isomer of hydroxylamine,
117 NH_3OH^+, with acetic acid involves a high activation barrier
118 (more than 27 kcal mol^{-1} at the CCSD(T) level). Only the
119 higher energy isomer, $NH_2OH_2^+$, led to a sensibly lower energy
120 barrier (about 2.3 kcal mol^{-1} at the CCSD(T) level).
121 Nevertheless, an estimate of the reaction coefficient at low
122 temperatures gave very low values. Therefore, it seemed that
123 precursors of interstellar glycine could not be efficiently
124 produced from the reactions of hydroxylamine-derived ions
125 with acetic acid.
126   Recently, Jeanvoine et al.[26] have investigated the dynamics
127 of the above-mentioned reactions. The authors concluded that
128 both tautomers of protonated hydroxylamine were able to
129 react with neutral acetic acid under gas-phase conditions, given

130 that some translational energy is provided. However, even
131 though reaction products had a mass−overcharge ratio, m/z
132 76, they did not have the structure of protonated glycine, but a
133 distribution of isomeric structures all different from protonated
134 glycine was found. These simulation results suggested that
135 astrophysicists should look for spectroscopic signatures of
136 these glycine isomers in the ISM, eventually.
137   In the present work, following Jeanvoine et al.'s[26]
138 conclusions, we have carried out a computational study of
139 the potential energy surfaces (PES) corresponding to the
140 reactions of formation of different products, all of them with
141 mass−overcharge ratio, m/z 76, and $[H_6C_2O_2N]^+$ molecular
142 formula (denoted as P1−P8). These products together with a
143 water molecule are obtained from the reaction of protonated
144 hydroxylamine and acetic acid. For each one of the reaction
145 products we provide structural data and spectroscopic
146 properties that could guide their possible search in the ISM.
147 In addition, we will also give information for their neutral
148 counterparts, with $[H_5C_2O_2N]$ molecular formula and denoted
149 as P1N−P8N, with the aim being to aid their laboratory or
150 astronomical detection by radioastronomy or infrared (IR)
151 spectroscopy as well as to analyze the behavior of these isomers
152 upon protonation.
153   The stability of different isomers of neutral and protonated
154 glycine was previously computed[27] at a highly correlated
155 coupled cluster level using the geometry and zero-point
156 vibrational energy (ZPE) obtained through density functional
157 theory. Some of the isomers considered in that study are
158 among the species included in both the neutral and protonated
159 systems analyzed in the present work. In this regard, it should
160 be remarked that our main goal here will not be to carry out an
161 exhaustive study for the most stable isomers of protonated and
162 neutral glycine; otherwise, it will be to provide structural and
163 spectroscopic information for the isomers of protonated
164 glycine concerned with the chemical dynamics simulations
165 study.[26] We will focus our attention on the formation processes
166 of the most abundant products found in the chemical dynamics
167 simulation study[26] of the reaction between acetic acid and
168 hydroxylamine. Nevertheless, we have carried out a compre-
169 hensive structural and spectroscopic description for all of the
170 isomers of protonated (P1−P8) and neutral (P1N−P8N)
171 glycine with the aim to aid their laboratory or astronomical
172 detection by radioastronomy or infrared (IR) spectroscopy.
173   To the best of our knowledge, among the neutral isomers
174 studied in the present work, only methyl carbamate
175 (CH_3OCONH_2) has been tentatively searched for in the hot
176 molecular cloud W51e2 and in the intermediate mass protostar
177 IRAS21391 + 58502.[28] Grooner et al.[29] studied its millimeter-
178 and sub-millimeter-wave spectrum providing rotational data in
179 a wide frequency range. What's more, glycolamide
180 ($HOCH_2CONH_2$) has also been characterized by free jet
181 millimeter-wave spectroscopy in the 60−78.3 GHz frequency
182 range in combination with a computational study.[30] To the
183 best of our knowledge, neither structural nor spectroscopic
184 information is available for the rest of the neutral species.

2. COMPUTATIONAL METHODS

185 The geometries of all the species (reactants, intermediates,
186 transition states, and products) studied in this work were first
187 optimized using the density functional theory (DFT) within
188 the hybrid B3LYP formalism[31,32] coupled with the correlation-
189 consistent polarized valence triple-ζ, cc-pVTZ basis set.[33,34]
190 Subsequently, structures were optimized at the second-order
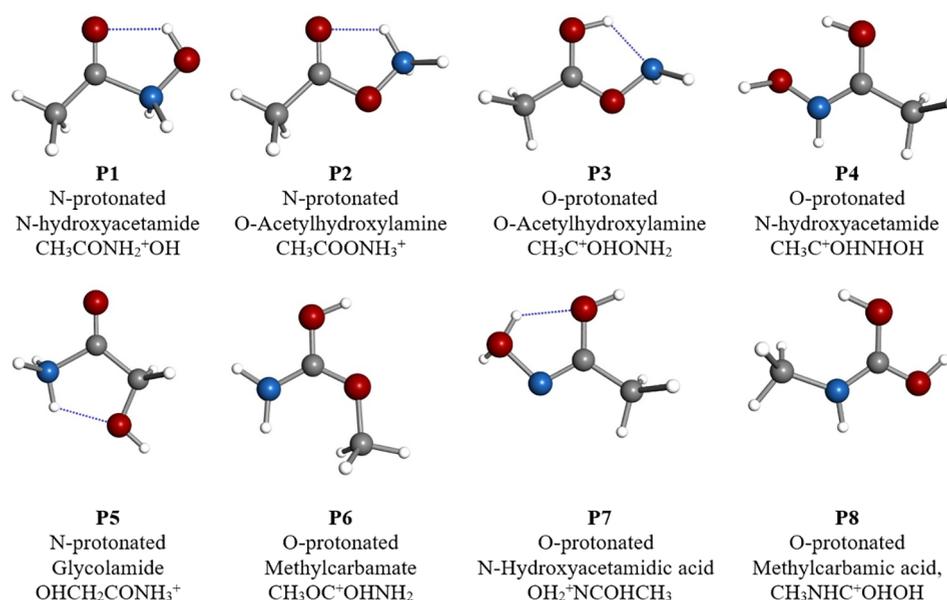
Figure 1. Chemical structures of $[H_6C_2O_2N]^+$ (**P1–P8**) isomers optimized at MP2/aug-cc-pVTZ level of theory.

Møller−Plesset level[35] in conjunction with the Dunning's aug-cc-pVTZ (correlation-consistent polarized valence triple-ζ including diffuse functions) basis set.[33,36] On each fully optimized structure, harmonic vibrational frequencies were calculated. This allows one to estimate the zero-point vibrational energy as well as to verify the nature of the stationary points located on the PES, either a true minimum with all vibrational frequencies real or a transition state (TS) with one of the frequencies, and just one, imaginary. To aid in a possible experimental identification by IR spectroscopy, we have computed anharmonic vibrational frequencies for both the protonated isomers: $[H_6C_2O_2N]^+$ species, and their neutral counterparts, $[H_5C_2O_2N]$ species. Anharmonic frequencies were computed at the MP2 level of theory using the second-order perturbation treatment (VPT2).[37] The treatment includes a full cubic force field (CFF) and semidiagonal quartic force constants. In addition, vibration−rotation interaction constants can also be evaluated, from the CFF calculations, allowing for correction of rotational constants, including vibrational effects.

In order to compute more accurate energies, we carried out coupled-cluster calculations. Specifically, the coupled-cluster single and double excitation model augmented with a noniterative triple excitation correction, CCSD(T),[38] was used in conjunction with the aug-cc-pVTZ basis set[33,36] on the MP2/aug-cc-pVTZ optimized geometries. The intrinsic reaction coordinate (IRC) technique[39,40] was used to check the connections between transition-state structures and adjacent minima.

The GAUSSIAN16[41] package of programs was used for all quantum calculations except for the computation of anharmonic corrections. For this purpose, the CFOUR[42] package was employed.

3. RESULTS AND DISCUSSION

According to the Bohme et al.'s experiments,[15] both isomers of protonated hydroxylamine (the most stable one, NH_3OH^+, and the high-energy $NH_2OH_2^+$) could be obtained in the protonation process of hydroxylamine using CH_5^+ as protonating agent. The energy barrier corresponding to the $NH_3OH^+ \rightarrow NH_2OH_2^+$ isomerization process is 50.71 kcal/mol at the CCSD(T) level of theory; consequently, both isomers, NH_3OH^+ and $NH_2OH_2^+$, could coexist when hydroxylamine is protonated. Neither of them react with H_2 under space conditions[43] and therefore both, if present in the interstellar medium, should be able to react with other molecules such as acetic acid.

In principle, acetic acid may react with both isomers of protonated hydroxylamine to produce protonated glycine and water, although other different products also with $[H_6C_2O_2N]^+$ molecular formula could be formed. Both processes can be summarized as follows:

$$NH_3OH^+ + CH_3COOH \rightarrow [H_6C_2O_2N]^+ + H_2O \qquad (1)$$

$$NH_2OH_2^+ + CH_3COOH \rightarrow [H_6C_2O_2N]^+ + H_2O \qquad (2)$$
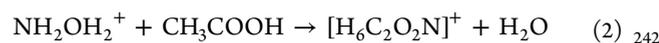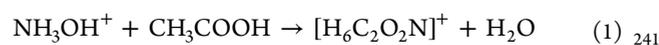
Given the spin multiplicity of the reactants, $NH_3OH^+(^1A')$, $NH_2OH_2^+$ (^1A), and CH_3COOH ($^1A'$), the reaction takes place on the singlet potential energy and all of the products are in their singlet electronic state (^1A).

3.1. Stability and Formation Processes of Protonated Glycine Isomers. In the dynamics simulations study by Jeanvoine et al.,[26] eight products, denoted as P1−P8, are obtained from the reaction of protonated hydroxylamine with acetic acid. The chemical structures of the P1−P8 reaction products are schematized in Figure 1. Before computation of reaction energies, we performed a detailed conformational analysis, for each one of the P1−P8 reaction products. It should be noted that, in the case of P1 and P3 products, we have found lowest lying conformational structures including intramolecular hydrogen bonds that are somewhat different from those considered in the work by Jeanvoine et al.[26]

In Table 1, we collect the relative energies, with respect to reactants, of the possible products that can be formed in the reaction between either NH_3OH^+ or $NH_2OH_2^+$ and CH_3COOH computed at different levels of theory. At the

Table 1. Relative Energies (Referred to Reactants), Including Zero Point Corrections, in kcal mol^{-1}, Obtained at Different Levels of Theory, for the Reaction between Protonated Hydroxylamine and Acetic Acid Yielding Protonated Glycine (GlyH$^+$) and Its Structural Isomers (P1–P8)

reacn[a]	B3LYP[b]	MP2[c]	CCSD[d]	CCSD(T)[e]
GlyH$^+$ + H$_2$O	−51.77	−59.12	−56.08	−56.29
GlyH$^+$ + H$_2$O	−76.59	−85.41	−83.62	−81.69
P8 + H$_2$O	−50.87	−54.86	−53.66	−52.86
P8 + H$_2$O	−75.69	−81.15	−81.20	−78.26
P6 + H$_2$O	−48.56	−51.38	−50.70	−49.88
P6 + H$_2$O	−73.38	−77.67	−78.24	−75.28
P5 + H$_2$O	−31.09	−38.13	−35.75	−36.02
P5+ H$_2$O	−55.91	−64.43	−63.30	−61.41
P4 + H$_2$O	−11.49	−12.74	−12.84	−12.83
P4+ H$_2$O	−36.31	−39.03	−40.38	−38.23
P2+ H$_2$O	−8.64	−11.86	−9.68	−10.95
P2 + H$_2$O	−33.46	−38.15	−37.23	−36.35
P3 + H$_2$O	−6.66	−7.59	−7.62	−8.38
P3 + H$_2$O	−31.48	−33.89	−35.16	−33.78
P1 + H$_2$O	5.42	0.89	2.71	1.52
P1 + H$_2$O	−19.41	−25.40	−24.83	−23.88
P7 + H$_2$O	15.85	14.60	14.43	13.29
P7 + H$_2$O	−8.97	−11.69	−22.54	−12.11

[a]The first entry refers to the NH$_3$OH$^+$ + CH$_3$COOH reaction and the second one to the NH$_2$OH$_2^+$ + CH$_3$COOH reaction. [b]Electronic energy calculated at the B3LYP/cc-pVTZ. [c]Electronic energy calculated at the MP2/aug-cc-pVTZ levels. [d]Electronic energy calculated at the CCSD/aug-cc-pVTZ//MP2/aug-cc-pVTZ level. [e]Electronic energy calculated at the CCSD(T)/aug-cc-pVTZ// MP2/aug-cc-pVTZ level.

CCSD(T) level of theory, hydroxylamine protonated in its oxygen atom, NH$_2$OH$_2^+$, was found to lie 25.4 kcal mol^{-1} higher in energy than the most stable isomer, NH$_3$OH$^+$. Thus, this value will be the difference of the reaction energies of processes 2 and 1 computed at this level of theory.

Excepting for the formation of the P1 (N-protonated N-hydroxyacetamide, CH$_3$CONH$_2^+$OH) and P7 (O-protonated N-hydroxyacetamidic acid, CH$_3$COHNOH$_2^+$) products from the reaction of NH$_3$OH$^+$ with acetic acid, all reactions studied including those giving protonated glycine are exothermic processes. The most favorable process, from thermodynamic arguments, is the formation of protonated glycine (GlyH$^+$, NH$_3^+$CH$_2$COOH). However, the P8 (O-protonated methyl-carbamic acid, CH$_3$NHC(OH)$_2^+$) and the P6 (O-protonated methylcarbamate, CH$_3$OC(OH)$^+$NH$_2$) products were found to be very close in energy to the most stable isomer (3.43 and 6.41 kcal mol^{-1}, respectively, at the CCSD(T) level). The P5 (N-protonated glycolamide, HOCH$_2$CONH$_3^+$) product was located 20.28 kcal mol^{-1} (at the CCSD(T) level) above protonated glycine, and the remaining reaction products were predicted to lie more than 40 kcal mol^{-1} above protonated glycine.

Regardless of the level of theory used, the stability order of the isomers with the [H$_6$C$_2$O$_2$N]$^+$ molecular formula studied in the present work at the CCSD(T)/aug-cc-pVTZ level is (">" means more stable than):

$$\text{GlyH}^+ > \text{P8} > \text{P6} > \text{P5} > \text{P4} > \text{P2} > \text{P3} > \text{P1} > \text{P7}$$
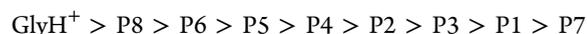
If a comparison is made among the results obtained at a different level of theory, we found a stabilization of the P8 and P6 isomers when B3LYP methodology is employed. At this level of theory, protonated glycine and the P8 isomers are
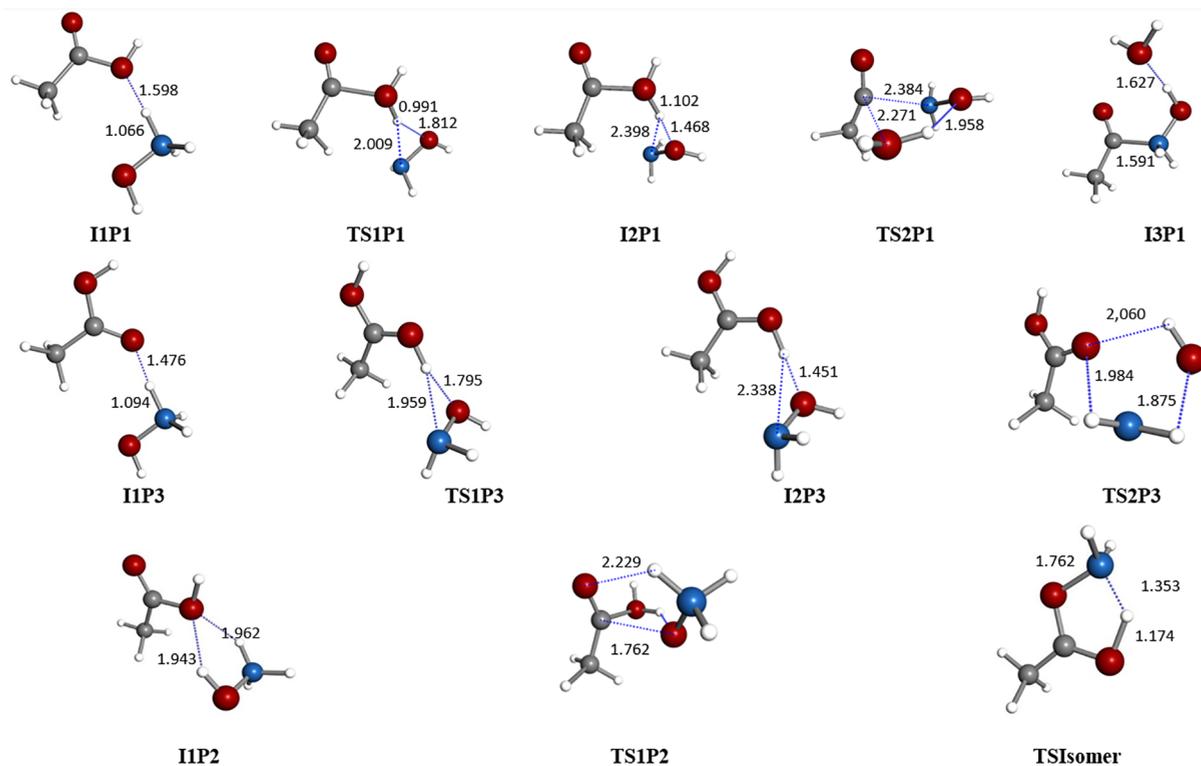

Figure 2. Intermediates and transition states involved on the reaction of formation of the P1–P3 isomers. Geometries are optimized at the MP2/aug-cc-pVTZ level of theory. Bond lengths are given in Angstroms.
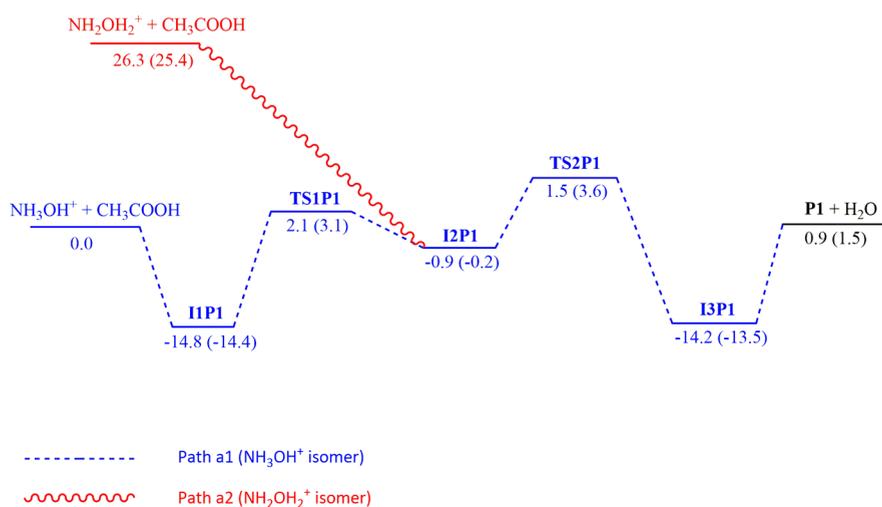
Figure 3. Energy profile, in kcal mol^{-1}, for the reactions of protonated hydroxylamine with acetic acid producing **P1** computed at the MP2/aug-cc-pVTZ and CCSD(T)/aug-cc-pVTZ (in parentheses) levels of theory. Zero-point vibrational energy computed at the MP2/aug-cc-pVTZ level is included.
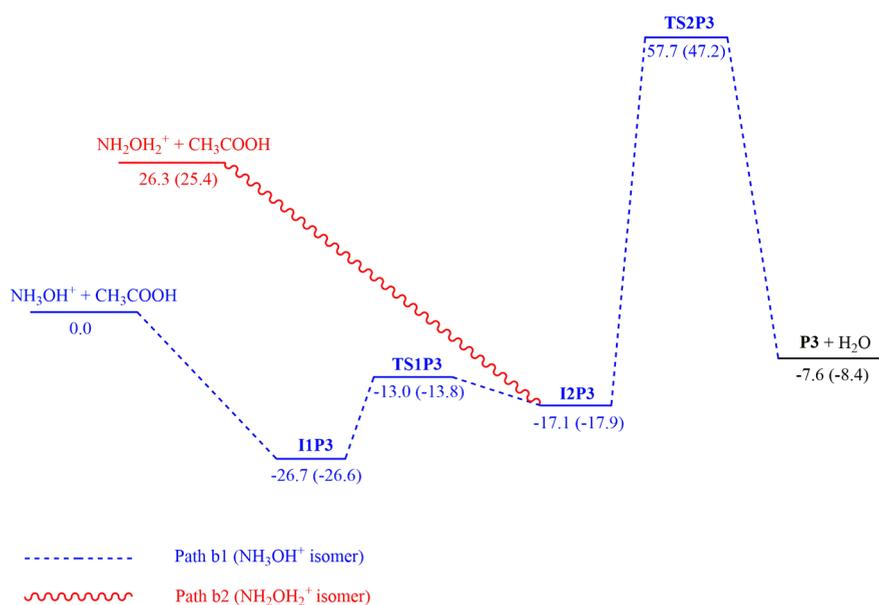

Figure 4. Energy profile, in kcal mol^{-1}, for the reactions of protonated hydroxylamine with acetic acid producing **P3** computed at the MP2/aug-cc-pVTZ and CCSD(T)/aug-cc-pVTZ (in parentheses) levels of theory. Zero-point vibrational energy computed at the MP2/aug-cc-pVTZ level is included.

almost isoenergetic, with GlyH$^+$ being slightly preferred by 0.9 kcal mol^{-1}. On the other hand, the CCSD(T) level tends to predict lower relative energies than the MP2 one.

A large energy difference was found between the two ends of the isomeric system, where protonated glycine, GlyH$^+$ (the most stable) and P7 (the less stable) differ by approximately 70 kcal mol^{-1}. This difference could be expected, and it mainly arises from the different chemical natures of the isomers. The multiple topological dispositions of the 11 atoms that make up the different structures allow one to generate species with different functional groups. In addition, the arrangement of the NH and OH groups leads to a wide range of possibilities for the formation of intramolecular hydrogen bonds that significantly stabilize this chemical system.

The relative stabilities of protonated glycine isomers were previously computed at the B3LYP/6-311G(d,p) level of theory.[27] From that study, protonated glycine was predicted to be the most stable isomer of the family with the CH$_3$NHC-(OH)$_2^+$ (P8) and the CH$_3$OC(OH)$^+$NH$_2$ (P6) isomers located 2.2 and 4.7 kcal mol^{-1}, respectively, higher in energy. Other isomers were found lower in energy than the P5 product; however, as it was already mentioned in the introduction, we will focus mainly on the products considered in the chemical dynamics simulations work.[26]

Even though protonated glycine is the most stable species among [H$_6$C$_2$O$_2$N]$^+$ molecular formula species, the chemical dynamics simulations study[26] of the reaction between protonated hydroxylamine and acetic acid found that P1 and P2 products were the most abundant isomers. It should be noted that these products are located 57.81 and 47.91 kcal mol^{-1}, respectively, at the CCSD(T) level of theory, higher in energy than protonated glycine. Only a small number of P3
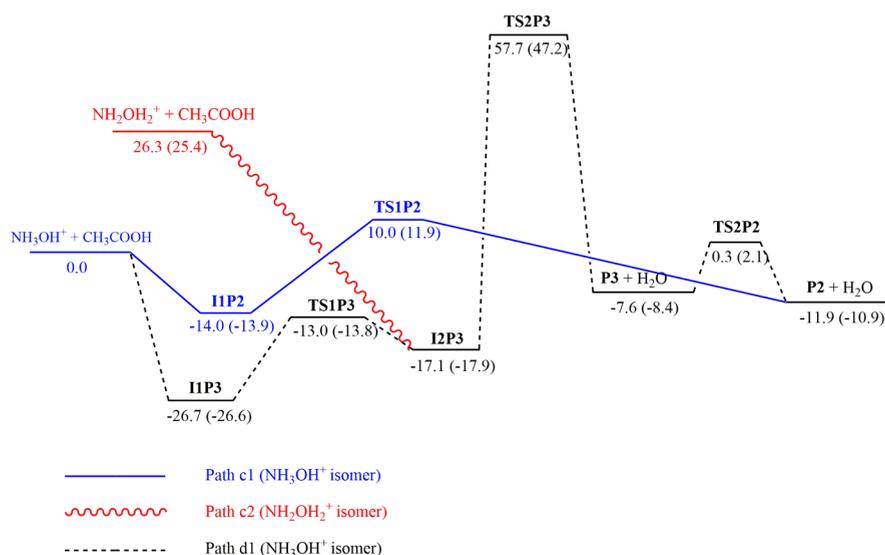
Figure 5. Energy profile, in kcal mol^{-1}, for the reactions of protonated hydroxylamine with acetic acid producing **P2** and **P3** computed at the MP2/aug-cc-pVTZ and CCSD(T)/aug-cc-pVTZ (in parentheses) levels of theory. Zero-point vibrational energy computed at the MP2/aug-cc-pVTZ level is included.

and P5 products were observed at the two temperatures (5 and 300 K) considered in that work.[26] Therefore, it should be useful to carry out a full exploration of the PES, to analyze the feasibility of the reactions studied as a source of the P1−P3 species in the interstellar medium. Given the conditions of interstellar medium, essentially low temperatures and low densities, interstellar plausible reactions should be exothermic and barrier free processes.

Figure 2 depicts the MP2/aug-cc-pVTZ optimized geometries for the intermediate species and transition states, with $[H_8C_2O_3N]^+$ molecular formula, involved in the formation process of the P1−P3 isomers. The energy profiles for these reactions computed at MP2 and CCSD(T) levels of theory are represented in Figures 3−5. In these representations, the energy of reactants is taken as a reference and the notations I1PX, I2PX, ... and TS1PX, TS2PX, ... (X = 1, 2, 3) are used for naming intermediates and transition states, respectively, involved in the corresponding reactions. As can be inferred from the figures, in general, a good agreement between the results obtained with the MP2 and CCSD(T) methodologies was found.

The energy profiles for the reactions of formation of the P1 isomer are shown in Figure 3. When the most stable isomer of protonated hydroxylamine, NH_3OH^+, is considered, the reaction starts with the formation of the I1P1 intermediate, which is the result of the interaction between the hydroxylic oxygen of acetic acid with one of the hydrogen atoms of the NH_3 group of protonated hydroxylamine. The exothermic formation of this first intermediate (14.4 kcal mol^{-1} at the CCSD(T) level) produces an energy reservoir that is used as the reaction proceeds toward the products. Once I1P1 is formed, a hydrogen migration from nitrogen to oxygen takes place through the TS1P1 transition state which is located 3.1 kcal mol^{-1} (1560 K) above reactants (at the CCSD(T)) level) giving the I2P1 intermediate. This intermediate evolves to the I3P1 intermediate through the TS2P1 transition state which is located, 3.6 kcal mol^{-1} (1812 K), at the CCSD(T) level, above reactants. In the TS2P1 transition state, a water molecule is coordinated to both NH_2OH and the highly electrophilic ion

$COCH_3^+$. Thus, when the NH_2 group is properly oriented, a N−C bond is formed, giving the I3P1 intermediate. This intermediate finally evolves to the formation of the P1 product and a water molecule. The process can be summarized as follows:

path a1:

$$NH_3OH^+ + CH_3COOH \rightarrow I1P1 \xrightarrow{\text{TS1P1}} I2P1 \xrightarrow{\text{TS2P1}} I3P1 \rightarrow \textbf{P1} + H_2O$$
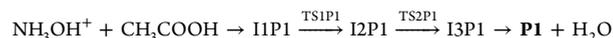
As can be seen in Figure 3, the global process is slightly endothermic (ΔE = 1.5 kcal mol^{-1} at the CCSD(T) level) and has a small but non-negligible activation barrier of 3.6 kcal mol^{-1} (1812 K) at the CCSD(T) level of theory. This barrier precludes this mechanism from taking place in the interstellar medium.

The first step in the mechanism of the formation of the P1 product from the less stable isomer of protonated hydroxylamine is the direct interaction between one of the hydrogen atoms bonded to oxygen of $NH_2OH_2^+$ and the hydroxylic oxygen of CH_3COOH giving the I2P1 intermediate. This complex finally evolves, through TS2P1, to produce P1 and H_2O as it is schematized in path a2:

path a2:

$$NH_2OH_2^+ + CH_3COOH \rightarrow I2P1 \xrightarrow{\text{TS2P1}} I3P1 \rightarrow \textbf{P1} + H_2O$$
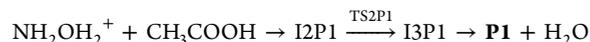
Pathway a2 is a clearly exothermic process (ΔE = −23.9 kcal mol^{-1} at the CCSD(T) level) with no net activation barrier since now the TS2P1 transition state lies 21.8 kcal mol^{-1} below reactants. Therefore, the formation of the P1 isomer could be feasible under interstellar conditions from the reaction of the less stable isomer of protonated hydroxylamine and acetic acid.

We will consider in advance the analysis of the PES corresponding to the formation of the P2 isomer because the process of formation of the P2 isomer can be derived from that of the P3 product.

Regarding formation of the P3 isomer, depicted in Figure 4, the mechanism of the reaction, involving the most stable isomer of protonated hydroxylamine, starts with the approach of one of the hydrogen atoms bonded to the nitrogen of

NH_3OH^+ to the carbonyl oxygen of acetic acid, giving rise to the I1P3 intermediate. Once I1P3 is obtained, a proton transfer from the NH_3 group to the carbonylic oxygen, through the TS1P3 transition state, occurs forming the I2P3 complex. As can be seen from Figure 4, TS1P3 is located lower in energy than the reactants (-13.8 kcal mol^{-1} at the CCSD(T) level). From an appropriate spatial arrangement of atoms in the I2P3 intermediate, a N—O bond cleavage and a simultaneous approach of the NH_2 group to the carbonyl oxygen takes place through the TS2P3 transition state which is located 47.2 kcal mol^{-1} (23752 K) above reactants (at the CCSD(T) level). This concerted process will eventually result in the formation of P3. This process can be summarized as

path b1:

$$NH_3OH^+ + CH_3COOH \rightarrow I1P3 \xrightarrow{TS1P3} I2P3 \xrightarrow{TS2P3} \textbf{P3} + H_2O$$

From this energy profile it seems that production of the P3 isomer from the lowest lying isomer of protonated hydroxyl-amine even though being an exothermic process ($\Delta E = -8.4$ kcal mol^{-1} at the CCSD(T) level) involves a large energy barrier (23752 K), since TS2P3 lies clearly higher in energy than reactants and it will not be feasible under interstellar conditions.

When the high-energy isomer of protonated hydroxylamine is considered, the reaction starts with the direct approach of one of the hydrogen atoms bonded to oxygen of $NH_2OH_2^+$ to the carbonylic oxygen of CH_3COOH giving the I2P3 intermediate. From this intermediate, as in the b1 pathway, the P3 isomer can be obtained from the migration of the NH_2 group and subsequent elimination of a water molecule through the TS2P3 transition state. TS2P3 is now located 21.8 kcal mol^{-1} (10970 K) above reactants at the CCSD(T) level. The process can be represented as

path b2:

$$NH_2OH_2^+ + CH_3COOH \rightarrow I2P3 \xrightarrow{TS2P3} \textbf{P3} + H_2O$$
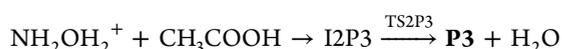
Therefore, the formation of the P3 isomer from the reaction of the less stable isomer of protonated glycine and acetic acid is an exothermic process ($\Delta E = -33.8$ kcal mol^{-1}); however, a net activation barrier of 21.8 kcal mol^{-1} was found, and this process will not be allowed under interstellar conditions.

It should be noted that the PES for the P3 isomer was previously studied[44] in an experimental and theoretical work using the CBS-QB3 complete basis set model chemistry.[45] From that study, the existence of a relationship with glycolaldehyde through a dissociative process is suggested.

In Figure 5 the PES corresponding to the formation of the P2 isomer from the two isomers of protonated hydroxylamine is schematized. If the reaction is initiated from NH_3OH^+, the mechanism starts with a concerted approach between both one of the hydrogen atoms bonded to nitrogen and the hydroxylic hydrogen of NH_3OH^+ to the hydroxylic oxygen of CH_3COOH giving the I1P2 intermediate. This intermediate evolves toward the products formation (P2 + H_2O) through the TS1P2 transition state. In this transition state, the hydrogen atom of the hydroxyl group of NH_3OH^+ is transferred to the hydroxylic oxygen of CH_3COOH, preforming a water molecule. Simultaneously, the highly reactive oxygen atom of NH_3O group interacts with the carbonyl carbon atom of acetic acid generating the P2 product in a concerted process

where a water molecule is released. The process can be schematized as follows:

path c1:

$$NH_3OH^+ + CH_3COOH \rightarrow I1P2 \xrightarrow{TS1P2} \textbf{P2} + H_2O \quad (c1)$$
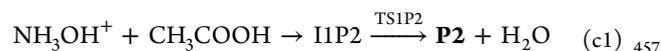
As can be seen from Figure 5, the reaction of formation of the P2 isomer, from the lowest lying isomer of protonated hydroxylamine through the c1 pathway, is an exothermic process ($\Delta E = -10.9$ kcal mol^{-1} at the CCSD(T) level) that involves a significant energy barrier since TS1P2 lies 11.9 kcal mol^{-1} (at the CCSD(T) level) than the reactants.

If we compare the b1 and c1 pathways, it can be seen that in the former additional energy is required to release the hydroxylic hydrogen of NH_3OH^+, whereas in the latter pathway a most favorable proton transfer occurs. This energy difference correlates with the energy associated with the following two processes:[26]

$$NH_3OH^+ \rightarrow NH_3O + H^+$$
$$(\Delta E = 211.6 \text{ kcal mol}^{-1} \text{ at the MP2/aug-cc-pVTZ level})$$

$$NH_3OH^+ \rightarrow NH_2OH + H^+$$
$$(\Delta E = 186.0 \text{ kcal mol}^{-1} \text{ at the MP2/aug-cc-pVTZ level})$$
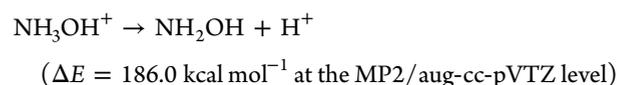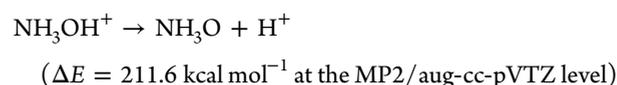
Another possibility for obtaining the P2 isomer, from NH_3OH^+, implies, first, the formation of the P3 product through the b1 pathway. Once P3 is obtained, second, the hydrogen atom migration from the oxygen atom to the nitrogen one, through the TS2P2 transition state, leads to the most stable isomer P2. This P3 → P2 isomerization process implies an energy barrier of 10.5 kcal mol^{-1} (at the CCSD(T) level). The overall process can be summarized as

path d1:

$$NH_3OH^+ + CH_3COOH \rightarrow I1P3 \xrightarrow{TS1P3} I2P3 \xrightarrow{TS2P3} \textbf{P3} + H_2O$$
$$\xrightarrow{TS2P2} \textbf{P2} + H_2O$$
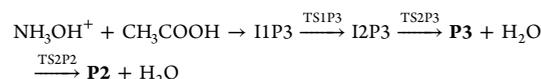
The TS2P2 transition state is located 2.1 kcal mol^{-1} higher in energy than reactants, and production of the P3 isomer involves a large energy barrier (23752 K); thus, the d1 path will have the same characteristics as the c1 pathway.

The reaction of formation of the P2 product from the highest energy isomer of protonated hydroxylamine starts with the interaction between one of the hydrogen atoms bonded to nitrogen in $NH_2OH_2^+$ and the carbonylic oxygen of acetic acid giving the I2P3 intermediate. This complex, following the b1 pathway, evolves to the P3 product, and then it isomerizes into the most stable P2 product through the TS2P2 transition state:

path c2:

$$NH_2OH_2^+ + CH_3COOH \rightarrow I2P3 \xrightarrow{TS2P3} \textbf{P3} + H_2O \xrightarrow{TS2P2} \textbf{P2} + H_2O$$
$$(c2)$$
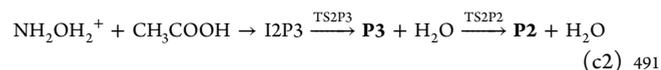
The process represented by the c2 pathway is clearly exothermic ($\Delta E = -36.3$ kcal mol^{-1} at the CCSD(T) level) but has a significant activation barrier (21.8 kcal mol^{-1} at the CCSD(T) level), and consequently it should not be relevant under interstellar conditions.

Our results show that the formation of P1, $CH_3CONH_2^+OH$, is the only favorable product from this reaction. It should be noted that protonated complex organic molecules (COMs) have not been yet detected in ISM; it

Table 2. Spectroscopic Parameters for the P1−P8 Isomers Computed at the MP2/aug-cc-pVTZ Level of theory

param	P1	P2	P3	P4	P5	P6	P7	P8
A^a	9767	10218	10478	10161	8524	9996	10140	10290
B	3858	4126	4162	4027	4192	4280	4043	4054
C	2859	3045	3085	2961	2906	3057	2957	29638
A_0^b	9652	10173	10419	10087	8423	9907	10046	10188
B_0	3799	4086	4141	4000	4174	4230	4008	4020
C_0	2819	3021	3068	2938	2896	3023	2930	2937
Δ_J^c	0.90	0.72	0.61	0.60	0.72	0.77	0.64	0.68
Δ_K	7.78	5.35	4.78	6.38	−27.02	2.02	6.57	2.00
Δ_{JK}	2.11	4.37	5.23	3.88	34.59	3.67	3.24	4.87
δ_J	0.23	0.19	0.16	0.16	0.18	0.22	0.16	0.18
δ_K	0.98	−5.66	−4.16	2.13	−14.68	2.74	2.06	2.17
X_a^d	1.60	0.26	5.40	−1.20	−0.43	1.02	6.10	2.04
$X_b − X_c$	1.10	0.35	−3.44	1.79	−0.10	5.51	0.05	4.40
$|\mu_a|/|\mu_b|/|\mu_c|^e$	1.4/3.8/0.0	4.7/1.4/0.0	1.5/0.7/0.0	0.7/2.1/1.1	1.3/3.2/0.1	0.8/1.7/0.0	1.4/1.8/1.5	1.4/0.4/0.0
P_c^f	3.046	3.020	2.919	2.208	3.84	1.655	1.957	1.624

^{a}A, B, and C represent the rotational constants of the equilibrium structure (in MHz). ^{b}A_0, B_0, and C_0 are the rotational constants of the ground vibrational state, $v = 0$ (in MHz). ^{c}Δ_J, Δ_K, Δ_{JK}, δ_J, and δ_K represent the quartic centrifugal distortion constants (in kHz). ^{d}X_a, X_b, and X_c represent the elements of the ^{14}N nuclear quadrupole coupling tensor (in MHz). ^{e}$|\mu_c|$ are the absolute values of the electric dipole-moment components (in D). ^{f}P_c is the planar inertial moment (in u A^2). Conversion factor: 505379.1 MHz^{-1} u A^2.


Figure 6. Chemical Structures of $[H_5C_2O_2N]$ isomers optimized at MP2/aug-cc-pVTZ level of theory

seems that they could evolve to neutral species by dissociative recombination. Therefore, the neutral isomer, OHNHCOCH₃, might be a candidate molecule to be searched for in the interstellar medium.

3.2. Structure and Spectroscopic Parameters of $[H_6C_2O_2N]^+$ and $[H_5C_2O_2N]$ Isomers. Structural data for the $[H_6C_2O_2N]^+$ isomers are given as Supporting Information, in Table S1. In Table 2, we provide the relevant spectroscopic parameters to rotational spectroscopy, together with computed dipole-moment components along their principal inertial axes, for the P1−P8 isomers. Equilibrium rotational constants (A, B, C) were computed at the MP2/aug-cc-pVTZ level, and the corresponding rotational constants for the ground vibrational state were calculated from vibration−rotation coupling constants and degeneracy factors for the vibrational modes. We have also included in the table centrifugal distortion parameters in the symmetrically reduced Hamiltonian (Δ_J, Δ_K, Δ_{JK}, δ_J, and δ_K). $[H_6C_2O_2N]^+$ isomers possess one nucleus with the quadrupole moment, ^{14}N ($I = 1$). The interaction at the nucleus of this quadrupole moment with the electric field gradient created by the rest of the molecular charges causes the coupling of the nuclear spin moments to the overall rotational momentum. Hence, each rotational transition of P1−P8 isomers carries the nuclear quadrupole hyperfine pattern expected for the presence of the ^{14}N nucleus, giving rise to a complex hyperfine pattern. Thus, in Table 2, the elements of the ^{14}N nuclear quadrupole coupling tensor (X_a, X_b, and X_c) are given.

Planar moments of inertia, P_c, have been also included in Table 2. They can be obtained from rotational constants through the relation $P_c = h/(16\pi^2)(-1/A_0 + 1/B_{<0} + 1/C_0)$ and represent the mass distribution outside the ab inertial plane. As can be seen in Table 2, the planar moments for the P1−P8 isomers are, in all cases, relatively significant in magnitude and different from zero indicating that all P1−P8 isomers are not entirely rigid nor planar structures. On the other hand, the values of the computed dipole moments are high enough to allow for the observation of their corresponding rotational spectra using standard micro- and millimeter-wave spectroscopy instruments.

All reaction products were predicted to be asymmetric tops. This characteristic together with the presence of one ^{14}N nucleus with a quadrupole moment ($I = 1$) results in a complex rotational spectrum.

To help in the possible identification of P1−P8 isomers in the gas phase through IR spectroscopy, in Table S2 of the Supporting Information, we give their predicted MP2/aug-cc-pVTZ harmonic and anharmonic vibrational frequencies. For all of the P1−P8 isomers, anharmonic frequencies are lower than the corresponding harmonic ones and the largest differences between harmonic and anharmonic frequencies were found, in general, in the frequencies corresponding to stretching modes.

Once P1−P8 ionic species were studied, the next step was to obtain spectroscopic information for the corresponding neutral species denoted as P1N−P8N. All of them are structural isomers of glycine and have $[H_5C_2O_2N]$ molecular formula. In this case, six different chemical species were analyzed, since both the P1N and P4N isomers and the P2N and P3N isomers converge, respectively, in the same neutral species (P1N = P4N, P2N = P3N). The six isomeric species studied together with neutral glycine are presented in Figure 6.

Again, for each isomer a previous conformational analysis was performed. In Table 3, the relative energies for the most

Table 3. Relative Energies, Including Zero Point Corrections, in kcal mol⁻¹, for Glycine (Gly) and Its Structural Isomers

isomer	B3LYP[a]	MP2[b]	CCSD[c]	CCSD(T)[d]
P8N	0.00	0.00	0.00	0.00
P6N	4.29	5.26	4.64	4.64
Gly	10.44	9.05	8.98	8.44
P5N	11.02	10.16	9.92	9.67
P2N	43.51	46.36	44.96	43.47
P1N	44.32	46.77	46.03	44.66
P7N	47.30	48.23	46.94	45.45

[a]Electronic energy calculated at the B3LYP/cc-pVTZ. [b]Electronic energy calculated at the MP2/aug-cc-pVTZ levels. [c]Electronic energy calculated at the CCSD/aug-cc-pVTZ//MP2/aug-cc-pVTZ level. [d]Electronic energy calculated at the CCSD(T)/aug-cc-pVTZ// MP2/aug-cc-pVTZ level.

stable conformers of the $[H_5C_2O_2N]$ isomers obtained at different levels of theory are given. As can be observed from the table, the stability order is not modified when going from the B3LYP level to the CCSD(T) one. The most stable structure is the P8N isomer (N-methylcarbamic acid, CH₃NHCOOH) and the less stable one corresponds to the P7N structure (N-hydroxyacetamidic acid, CH₃COHNOH). It should be noted that, among neutral isomers, glycine (Gly) is not the most stable species; it is situated in stability between P6N (methylcarbamate, CH₃OCONH₂) and P5N (glyco-lamide, HOCH₂CONH₂) isomers. Regardless of the level of calculation employed, the stability order of the isomers considered in this work with $[H_5C_2O_2N]$ molecular formula is (">" means more stable than):

P8N > P6N > Gly > P5N > P2N > P1N > P7N

The energetic difference between the ends of the series is now lower than in the protonated counterpart. The high-energy isomer, P7N, is 45.5 kcal mol⁻¹ (at the CCSD(T) level) higher in energy than the most stable one P8N.

Lattelais et al.[27] in their study of the isomers of glycine found that the most stable isomer was not glycine, but N-methylcarbamic acid (P8N). Following in energy were found methylcarbamate (P6N) and glycine (Gly), which are located

4.9 and 8.8 kcal mol⁻¹, respectively, higher in energy than the most stable isomer at the CCSD(T)/cc-pVQZ//B3LYP/6-311G(d.p) level.

Proton transfer processes are common in the interstellar medium; therefore, we have computed proton affinities for the neutral isomers, which are showen, at different level of theory, in Table 4. As can be seen from the table, the values of proton

Table 4. Proton Affinities, Including Zero Point Corrections, in kcal mol⁻¹, for $[H_5C_2O_2N]$ Isomers

reacn	B3LYP[a]	MP2[b]	CCSD[c]	CCSD(T)[d]
P8N + H⁺ → P8	201.37	196.44	200.67	199.15
P6N + H⁺ → P6	203.35	198.22	202.35	200.80
P5N + H⁺ → P5	192.60	189.87	192.69	191.97
P2N + H⁺ → P2	202.66	199.80	201.66	200.71
P2N + H⁺ → P3b	200.67	195.53	199.59	198.14
P1N + H⁺ → P 4d	206.31	201.12	205.89	203.78
P1N + H⁺ → P1b	189.40	187.46	190.33	189.43
P7N + H⁺ → P7a	181.95	175.21	180.86	178.45

[a]Electronic energy calculated at the B3LYP/cc-pVTZ. [b]Electronic energy calculated at the MP2/aug-cc-pVTZ levels. [c]Electronic energy calculated at the CCSD/aug-cc-pVTZ//MP2/aug-cc-pVTZ level. [d]Electronic energy calculated at the CCSD(T)/aug-cc-pVTZ// MP2/aug-cc-pVTZ level.

affinities are relatively high if comparison is made to those of some abundant interstellar molecules. For example, the proton affinities of H₂, CO, and C₂H₂ are 100, 143, and 152 kcal mol⁻¹, respectively. Therefore, neutral isomers should react quite easily in proton-rich interstellar media to give the corresponding protonated species.

As it was noted for the protonated systems, other isomers were found lower in energy than the P5N product, in the theoretical study of Lattelais et al.[27] However, we will only provide spectroscopic information for the neutral isomers derived from the products considered in the chemical dynamics simulations work.[26]

As Supporting Information, in Table S3, we give geometrical parameters for the $[H_5C_2O_2N]$ isomers.

Rotational spectroscopic parameters for neutral isomers are given in Table 5. As in their protonated counterparts, all neutral isomers are asymmetric tops and their rotational spectrum should show the quadrupole hyperfine pattern that can be expected for those of molecules with a ¹⁴N atom. Dipole moments values for the neutral isomers were high enough to allow for their characterization by micro- and millimeter-wave spectroscopy.

According to our calculations N-hydroxyacetamide (P1N), the neutral counterpart of the only protonated isomer which could be formed from the reaction of acetic acid and protonated hydroxylamine under interstellar conditions is an asymmetric rotor. In Figure 7, we present a prediction of the rotational spectra[46] in a large spectral range interesting for astrophysical use (40−200 GHz). Its rotational spectrum can be derived from the corresponding rotational constants and dipole-moment components in order to guide spectral searches. ¹⁴N nuclear quadrupole coupling tensor constants are also included in the predictions. This study, in combination with a plausible frequency modulation millimeter-wave spectroscopic work, should allow astrophysicists to search for N-hydroxyacetamide in the ISM using the available survey data from IRAM 30m, ARO, CARMA, ALMA, ...

Table 5. Spectroscopic Parameters for the $[H_5C_2O_2N]$ Isomers Computed at the MP2/aug-cc-pVTZ Level of theory

param	P1N	P2N	P5N	P6N	P7N	P8N
A^a	10600	10465	10449	10673	10114	10695
B	4140	4236	4077	4429	4133	4109
C	3045	3102	2987	3196	2988	3025
$A_0{}^b$	10529	10383	10361	10593	10012	10625
B_0	4099	4193	4015	4389	411	4063
C_0	3015	3073	2955	3164	2962	2989
$\Delta_J{}^c$	0.72	0.76	0.76	0.77	0.67	0.65
Δ_K	7.73	6.66	2.29	3.83	5.80	−5.15
Δ_{JK}	3.22	4.14	6.31	3.05	5.21	12.65
δ_J	0.19	0.21	0.20	0.21	0.17	0.17
δ_K	1.62	−0.29	2.050	2.39	3.16	−16.2
$X_a{}^d$	4.04	4.39	5.93	2.21	5.06	2.55
$X_b - X_c$	5.70	3.83	0.09	6.07	−3.55	6.59
$\lvert\mu_a\rvert/\lvert\mu_b\rvert/\lvert\mu_c\rvert^e$	1.7/2.7/0.8	0.8/1.1/1.3	3.2/3.0/0.0	0.1/2.2/0.6	2.5/0.0/0.0	1.2/2.2/0.0
$P_c{}^f$	1.835	2.373	1.812	1.564	1.365	1.436

^{a}A, B, and C represent the rotational constants of the equilibrium structure (in MHz). ^{b}A_0, B_0, and C_0 are the rotational constants of the ground vibrational state, v = 0 (in MHz). $^c\Delta_J$, Δ_K, Δ_{JK}, δ_J, and δ_K represent the quartic centrifugal distortion constants (in kHz). ^{d}X_a, X_b, and X_c represent the elements of the ^{14}N nuclear quadrupole coupling tensor (in MHz). $^e\lvert\mu_a\rvert$, $\lvert\mu_b\rvert$, and $\lvert\mu_c\rvert$ are the absolute values of the electric dipole-moment components (in D). ^{f}P_c is the planar inertial moment (in u A^2). Conversion factor: 505379.1 MHz^{-1} u A^2.
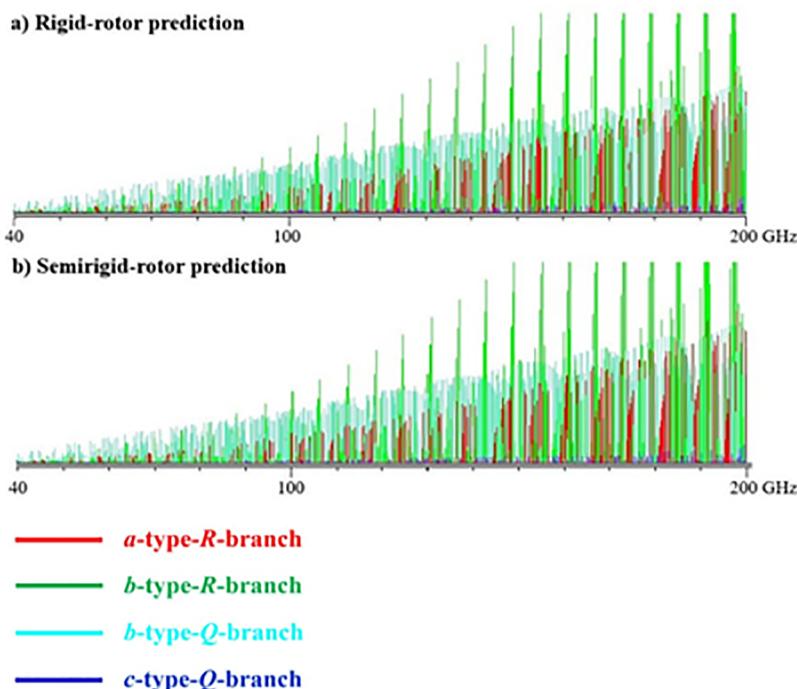

Figure 7. Calculated rotational spectra of *N*-Hydroxyacetamide (P1N) at room temperature. a) Rotational spectrum in the 40−200 GHz frequency region using a rigid-rotor approximation. b) Rotational spectrum in the 40−200 GHz frequency region using a semirigid-rotor approximation including quartic centrifugal distortion parameters in the symmetrically reduced Hamiltonian. SPCAT program[46] is used to predict frequencies and intensities from the parameters.

Finally, the calculated harmonic and anharmonic vibrational frequencies and IR intensities for the neutral isomers are given in Table S4 as Supporting Information. This information could be useful for their eventual detection in the gas phase through IR spectroscopy.

4. CONCLUSION

In this work, we have carried out a theoretical study of the possible products obtained from reaction between protonated hydroxylamine and acetic acid. These products have $[H_6C_2O_2N]^+$ molecular formula and are structural isomers of protonated glycine. In addition, their neutral counterparts, with $[H_5C_2O_2N]$ molecular formula have been analyzed.

For the $[H_6C_2O_2N]^+$ system, all levels of theory employed in this study predict protonated glycine as the lowest energy isomer with the P8 ($CH_3NHC(OH)_2$) and P6 ($CH_3OC-(OH)^+NH_2$) isomers close in energy, 3.43 kcal mol^{-1} and 6.41 kcal mol^{-1}, respectively, above protonated glycine at the CCSD(T) level.

All reaction processes that could form $[H_6C_2O_2N]^+$ isomers from the reaction between protonated hydroxylamine and acetic acid are exothermic except for those initiated by the

most stable isomer of protonated hydroxylamine which lead to the P1 ($CH_3CONH_2^+OH$) and P7 ($CH_3COHNOH_2^+$) isomers.

The study has been focused on the most abundant products, denoted as P1 ($CH_3CONH_2^+OH$), P2 ($CH_3COONH_3^+$), and P3 ($CH_3C(OH)^+ONH_2$), obtained from a previous[26] chemical dynamics simulations study on the reaction between protonated hydroxylamine and acetic acid. Thus, for these isomers a detailed analysis of the corresponding singlet potential energy surface has been performed. From the analysis of the potential energy surfaces, we can conclude that even if the reactions of formation of P2 and P3 isomers are exothermic processes, significant activation barriers were found in the paths leading to these products. The only exothermic process ($\Delta E = -23.9$ kcal mol^{-1} at the CCSD(T) level) with no net activation barrier was initiated by the high-energy isomer of protonated hydroxylamine, which leads to the P1 ($CH_3CONH_2^+OH$) isomer. Therefore, the formation of $CH_3CONH_2^+OH$ could be feasible under interstellar conditions from the reaction of the less stable isomer of protonated hydroxylamine and acetic acid. Consequently, from these results, the neutral isomer P1N (N-hydroxyacetamide, $CH_3CONHOH$) might be a candidate molecule to be searched for in the interstellar medium.

The relevant spectroscopic parameters to rotational spectroscopy, harmonic and anharmonic frequencies, and IR intensities are reported for $[H_6C_2O_2N]^+$ and $[H_5C_2O_2N]$ isomers. This information could aid in their laboratory characterization by micro- and millimeter-wave spectroscopy or astronomical search by radioastronomy or IR spectroscopy.

ASSOCIATED CONTENT

Supporting Information

The Supporting Information is available free of charge on the ACS Publications website at DOI: 10.1021/acsearthspacechem.9b00053.

Geometry optimized for P1−P8 isomers (Table S1), harmonic and anharmonic vibrational frequencies of P1−P8 isomers (Table S2), geometry optimized for P1N−P8N isomers (Table S3), and harmonic and anharmonic vibrational frequencies of P1N−P8N isomers (Table S4) (PDF)

AUTHOR INFORMATION

Corresponding Author

*E-mail: carmen.barrientos@uva.es.

ORCID

Antonio Largo: 0000-0003-4959-4850
Carmen Barrientos: 0000-0003-0078-7379

Notes

The authors declare no competing financial interest.

ACKNOWLEDGMENTS

REFERENCES

(1) Miller, S. L. A Production of Amino Acids under Possible Primitive Earth Conditions. *Science* **1953**, *117*, 528−529.

(2) Johnson, A. P.; Cleaves, H. J.; Dworkin, J. P.; Glavin, D. P.; Lazcano, A.; Bada, J. L. The Miller Volcanic Spark Discharge Experiment. *Science* **2008**, *322*, 404.

(3) Pizzarello, S. The Chemistry of Life's Origin: A Carbonaceous Meteorite Perspective. *Acc. Chem. Res.* **2006**, *39*, 231−237.

(4) Pizzarello, S.; Shock, E. The Organic Composition of Carbonaceous Meteorites: The Evolutionary Story Ahead of Biochemistry. *Cold Spring Harbor Perspect. Biol.* **2010**, *2*, a002105.

(5) Burton, A. S.; Stern, J. C.; Elsila, J. E.; Glavin, D. P.; Dworkin, J. P. Understanding Prebiotic Chemistry through the Analysis of Extraterrestrial Amino Acids and Nucleobases in Meteorites. *Chem. Soc. Rev.* **2012**, *41*, 5459−5472.

(6) Ruiz-Mirazo, K.; Briones, C.; de la Escosura, A. Prebiotic Systems Chemistry: New Perspectives for the Origins of Life. *Chem. Rev.* **2014**, *114*, 285−366.

(7) Snyder, L. E.; Lovas, F. J.; Hollis, J. M.; Friedel, D. N.; Jewell, P. R.; Remijan, A.; Ilyushin, V. V.; Alekseev, E. A.; Dyubko, S. F. A Rigorous Attempt to Verify Interstellar Glycine. *Astrophys. J.* **2005**, *619*, 914−930.

(8) Cunningham, M. R.; Jones, P. A.; Godfrey, P. D.; Cragg, D. M.; Bains, I.; Burton, M. G.; Calisse, P.; Crighton, N. H. M.; Curran, S. J.; Davis, T. M.; Dempsey, J. T.; Fulton, B.; Hidas, M. G.; Hill, T.; Kedziora-Chudczer, L.; Minier, V.; Pracy, M. B.; Purcell, C.; Shobbrook, J.; Travouillon, T. A Search for Propylene Oxide and Glycine in Sagittarius B2 (LMH) and Orion. *Mon. Not. R. Astron. Soc.* **2007**, *376*, 1201−1210.

(9) Jones, P. A.; Cunningham, M. R.; Godfrey, P. D.; Cragg, D. M. A Search for Biomolecules in Sagittarius B2 (LMH) with the AustraliaTelescope Compact Array. *Mon. Not. R. Astron. Soc.* **2007**, *374*, 579−589.

(10) Hollis, J. M.; Pedelty, J. A.; Snyder, L. E.; Jewell, P. R.; Lovas, F. J.; Palmer, P.; Liu, S.-Y. A Sensitive Very Large Array Search for SmallScale Glycine Emission Toward OMC-1. *Astrophys. J.* **2003**, *588*, 353−359.

(11) Altwegg, K.; Balsiger, H.; Bar-Nun, A.; Berthelier, J.-J.; Bieler, A.; Bochsler, P.; Briois, C.; Calmonte, U.; Combi, M. R.; Cottin, H.; De Keyser, J.; Dhooghe, F.; Fiethe, B.; Fuselier, S. A.; Gasc, S.; Gombosi, T. I.; Hansen, K. C.; Haessig, M.; Jäckel, A.; Kopp, E.; Korth, A.; Le Roy, L.; Mall, U.; Marty, B.; Mousis, O.; Owen, T.; Rème, H.; Rubin, M.; Sémon, T.; Tzou, C. Y.; Hunter Waite, J.; Wurz, P. Prebiotic Chemicals - Amino Acid and Phosphorus - in the Coma of Comet 67P/Churyumov-Gerasimenko. *Sci. Adv.* **2016**, *2*, No. e1600285.

(12) Ehrenfreund, P.; Bernstein, M.; Dworkin, J. P.; Sandford, S. A.; Allamandola, L. The Photostability of Amino Acids in Space. *Astrophys. J.* **2001**, *550*, L95−L99.

(13) Irvine, W. Extraterrestrial Organic Matter: A Review. *Origins Life Evol. Biospheres* **1998**, *28*, 365−383.

(14) Herbst, E. The Chemistry of Interstellar Space. *Chem. Soc. Rev.* **2001**, *30*, 168−176.

(15) Snow, J. L.; Orlova, G.; Blagojevic, V.; Bohme, D. K. Gas-Phase Ionic Syntheses of Amino Acids: β versus α. *J. Am. Chem. Soc.* **2007**, *129*, 9910−9917.

(16) Blagojevic, V.; Petrie, S.; Bohme, D. K. Gas-Phase Syntheses for Interstellar Carboxylic and Amino Acids. *Mon. Not. R. Astron. Soc.* **2003**, *339*, L7−L11.

(17) Mehringer, D. M.; Snyder, L. E.; Miao, Y.; Lovas, F. J. Detection and Confirmation of Interstellar Acetic Acid. *Astrophys. J.* **1997**, *480*, L71−L74.

(18) Remijan, A.; Snyder, L. E.; Liu, S.-Y.; Mehringer, D.; Kuan, Y.-J. Acetic Acid in the Hot Cores of Sagitarrius B2(N) and W51. *Astrophys. J.* **2002**, *576*, 264−273.

(19) He, J.; Vidali, G.; Lemaire, J.-M.; Garrod, R. T. Formation of Hydroxylamine on Dust Grains Via Ammonia Oxidation. *Astrophys. J.* **2015**, *799*, 49.

(20) Nishi, N.; Shinohara, H.; Okuyama, T. Photodetachment, Photodissociation, and Photochemistry of Surfacemolecules of Icy Solids Containing NH₃ and Pure H₂O Ices. *J. Chem. Phys.* **1984**, *80*, 3898–3910.

(21) Zheng, W.; Kaiser, R. I. Formation of Hydroxylamine (NH₂OH) in Electron-Irradiated Ammonia-Water Ices. *J. Phys. Chem. A* **2010**, *114*, 5251–5255.

(22) Congiu, E.; Fedoseev, G.; Ioppolo, S.; Dulieu, F.; Chaabouni, H.; Baouche, S.; Lemaire, J. L.; Laffon, C.; Parent, P.; Lamberts, T.; Cuppen, H. M.; Linnartz, H. No Ice Hydrogenation: A Solid Pathway to NH₂OH Formation in Space. *Astrophys. J., Lett.* **2012**, *750*, L12.

(23) Charnley, S. B.; Rodgers, S. D.; Ehrenfreund, P. Gas-Grain Chemical Models Of Star-Forming Molecular Clouds as Constrained by ISO and SWAS Observations. *Astron. Astrophys.* **2001**, *378*, 1024–1036.

(24) Jonusas, M.; Krim, L. A Possible Answer to the Mysterious Non-Detection of Hydroxylamine in Space: The Thermal Desorption Mechanism. *Mon. Not. R. Astron. Soc.* **2016**, *459*, 1977–1984.

(25) Barrientos, C.; Redondo, P.; Largo, L.; Rayón, V. M.; Largo, A. Gas-Phase Synthesis of Precursors of Interstellar Glycine: A Computational Study of the Reactions of Acetic Acid with Hydroxylamine and its Ionized and Protonated Derivatives. *Astrophys. J.* **2012**, *748*, 99.

(26) Jeanvoine, Y.; Largo, A.; Hase, W. L.; Spezia, R. Gas Phase Synthesis of Protonated Glycine by Chemical DynamicsSimulations. *J. Phys. Chem. A* **2018**, *122*, 869–877.

(27) Lattelais, M.; Pauzat, F.; Pilmé, J.; Ellinger, Y.; Ceccarelli, C. About the Detectability of Glycine in the Interstellar Medium. *Astron. Astrophys.* **2011**, *532*, A39.

(28) Demyk, K.; Wlodarczak, G.; Dartois, E. In *Semaine de l'Astrophysique Francaise*, SF2A-2004, Jun. 14–18, 2004, Paris, France; Combes, F., Barret, D., Contini, T., Meynadier, F., Pagani, L., Eds.; EDP-Sciences, Les Ulis, France, 2004; p 493.

(29) Groner, P.; Winnewisser, M.; Medvedev, I. R.; De Lucia, C.; Herbst, E.; Sastry, K. The Millimeter- and Submillimeter-Wave Spectrum of Methyl Carbamate [CH₃OC(:O)NH₂]. *Astrophys. J., Suppl. Ser.* **2007**, *169*, 28–36.

(30) Maris, A. On the Conformational Equilibrium of Glycolamide: A Free Jet Millimetre-Wave Spectroscopy and Computational Study. *Phys. Chem. Chem. Phys.* **2004**, *6*, 2611–2616.

(31) Becke, A. D. Density-Functional Thermochemistry. The Role of Exact Exchange. *J. Chem. Phys.* **1993**, *98*, 5648–5652.

(32) Lee, C.; Yang, W.; Parr, R. G. Development of the Colle-SalvettiCorrelation-Energy Formula into a Functional of the Electron Density. *Phys. Rev. B: Condens. Matter Mater. Phys.* **1988**, *37*, 785–789.

(33) Dunning, T. H. Gaussian Basis Sets for Use in Correlated Molecular Calculations. I. The Atoms Boron through Neon andHydrogen. *J. Chem. Phys.* **1989**, *90*, 1007–1023.

(34) Kendall, R. A.; Dunning, T. H., Jr.; Harrison, R. J. Electron Affinities of the First-Row Atoms Revisited. Systematic Basis Sets andWave Functions. *J. Chem. Phys.* **1992**, *96*, 6796–6806.

(35) Møller, C.; Plesset, M. Note on an Approximation Treatmentfor Many-Electron Systems. *Phys. Rev.* **1934**, *46*, 618–622.

(36) Woon, D. E.; Dunning, T. H. Gaussian Basis Sets for Use in Correlated Molecular Calculations. III. The Atoms Aluminium-through Argon. *J. Chem. Phys.* **1993**, *98*, 1358–1371.

(37) Barone, V. Anharmonic Vibrational Properties by a Full-yAutomated Second-Order Perturbative Approach. *J. Chem. Phys.* **2005**, *122*, 014108.

(38) Raghavachari, K.; Trucks, G. W.; Pople, J. A.; Head-Gordon, M. A Fifth-Order Perturbation Comparison of Electron Correlation-Theories. *Chem. Phys. Lett.* **1989**, *157*, 479–483.

(39) Gonzalez, C.; Schlegel, H. B. An Improved Algorithm for Reaction Path Following. *J. Chem. Phys.* **1989**, *90*, 2154–2161.

(40) Gonzalez, C.; Schlegel, H. B. Reaction Path Following in MassweightedInternal Coordinates. *J. Phys. Chem.* **1990**, *94*, 5523–5527.

(41) Frisch, M. J.; Trucks, G. W.; Schlegel, H. B.; Scuseria, G. E.; Robb, M. A.; Cheeseman, J. R.; Scalmani, G.; Barone, V.; Petersson, G. A.; Nakatsuji, H.; Li, X.; Caricato, M.; Marenich, A. V.; Bloino, J.; Janesko, B. G.; Gomperts, R.; Mennucci, B.; Hratchian, H. P.; Ortiz, J. V.; Izmaylov, A. F.; Sonnenberg, J. L.; Williams-Young, D.; Ding, F.; Lipparini, F.; Egidi, F.; Goings, J.; Peng, B.; Petrone, A.; Henderson, T.; Ranasinghe, D.; Zakrzewski, V. G.; Gao, J.; Rega, N.; Zheng, G.; Liang, W.; Hada, M.; Ehara, M.; Toyota, K.; Fukuda, R.; Hasegawa, J.; Ishida, M.; Nakajima, T.; Honda, Y.; Kitao, O.; Nakai, H.; Vreven, T.; Throssell, K.; Montgomery, J. A., Jr.; Peralta, J. E.; Ogliaro, F.; Bearpark, M. J.; Heyd, J. J.; Brothers, E. N.; Kudin, K. N.; Staroverov, V. N.; Keith, T. A.; Kobayashi, R.; Normand, J.; Raghavachari, K.; Rendell, A. P.; Burant, J. C.; Iyengar, S. S.; Tomasi, J.; Cossi, M.; Millam, J. M.; Klene, M.; Adamo, C.; Cammi, R.; Ochterski, J. W.; Martin, R. L.; Morokuma, K.; Farkas, O.; Foresman, J. B.; Fox, D. J. *Gaussian 16*, Revision B.01; Gaussian: Wallingford, CT, USA, 2016.

(42) Stanton, J. F.; Gauss, J.; Harding, M. E.; Szalay, P. G. *CFOUR, Coupled-Cluster Techniques for Computational Chemistry*, A Quantum Chemical Program Package; 2013.

(43) Largo, L.; Rayon, V. M.; Barrientos, C.; Largo, A.; Redondo, P. Stability of Protonated and Ionized Hydroxylamine in the Interstellar Medium. *Chem. Phys. Lett.* **2009**, *476*, 174–177.

(44) Jobst, K. J.; Ruttink, P. J. A.; Terlouw, J. K. The Remarkable Dissociation Chemistry of 2-Aminoxyethanol Ions NH₂OCH₂CH₂OH⁺ Studied by Experiment and Theory. *Int. J. Mass Spectrom.* **2008**, *269*, 165–176.

(45) Montgomery, J. A., Jr.; Frisch, M. J.; Ochterski, J. W.; Petersson, G. A. A complete basis set model chemistry. VII. Use of the Minimum Population Localization Method. *J. Chem. Phys.* **2000**, *112*, 6532–6542.

(46) Pickett, H. M. The Fitting and Prediction of Vibration-Rotation Spectra with Spin Interactions. *J. Mol. Spectrosc.* **1991**, *148*, 371–377.